Boosting silver loading and functionality in Clinoptilolite via tannic acid reduction: a comparative study of ionic and metallic silver for air purification

Materials Research Bulletin 204 (2026) 114305

Contents lists available at ScienceDirect

Materials Research Bulletin

journal homepage: www.elsevier.com/locate/matresbu

Research papers

Boosting silver loading and functionality in Clinoptilolite via tannic acid reduction: a comparative study of ionic and metallic silver for air purification

Francesca Gattucci, Mari Sofia Lallukka, Nadia Grifasi, Marco Armandi, Marco Piumetti, Marta Miola *

Department of Applied Science and Technology, Polytechnic of Turin, Corso Duca Degli Abruzzi, 24, 10129, Turin, Italy

ARTICLE INFO

Keywords:
Air purification
Natural zeolite clinoptilolite
Silver
Environmental catalysis
Antibacterial

ABSTRACT

Air purification is essential for protecting human health, as airborne pathogens and pollutants contribute to respiratory infections. Natural materials such as zeolites, particularly clinoptilolite, have attracted attention due to their high adsorption capacity and ion exchange properties, making them promising for air purification. This study investigates the functionalization of natural clinoptilolite with silver to enhance its catalytic and antibacterial performance using two green methods. The first involves ion exchange to introduce silver ions (Clino-Ag), while the second uses tannic acid to promote the formation of silver nanoparticles (Clino-AgNPs), keeping the precursor amount constant. The materials were characterized by FESEM, XRD, EDS, and STEM, while textural properties were analyzed via N_2 and CO_2 adsorption. Catalytic activity was tested for CO and ethylene oxidation, and antibacterial efficacy was evaluated using bacterial bioaerosols. Results showed that morphology influenced performance, with metallic silver providing superior catalytic activity, while both forms exhibited strong antibacterial properties.

1. Introduction

Air quality has significant health implications, particularly in indoor environments, where it can contain harmful chemicals, particulates, infectious agents, as well as pollen and other allergens [1]. In recent years, the COVID−19 pandemic has underscored the importance of addressing the transmission of viral pathogens, such as viruses, fungi, and bacteria. Diseases like measles, tuberculosis, severe acute respiratory syndrome (SARS), influenza, and rhinovirus are primarily spread through aerosol particles [2], with pathogen-containing saliva droplets released during speaking, coughing, or sneezing being carried by air currents [3].

In addition to viral pathogens, indoor air often contains atmospheric particulate matter (PM), which has a strong ability to adsorb toxic metals. These particles can be inhaled, causing harmful physiological effects, and have been linked to various diseases, including cardiovascular and respiratory conditions, as well as lung cancer [4]. The harmful effects of PM are also seen in microbial infections, as airborne microorganisms can attach to particles, facilitating the spread of infections [5].

Furthermore, volatile organic compounds (VOCs), commonly found in gas form, are produced by humans for domestic and commercial use, particularly in urban areas. High levels of VOC pollution are linked to vehicle emissions, industrial processes, waste decomposition, and solvent use [6]. VOCs undergo chemical transformations that result in the formation of reactive substances, contributing to pollution, climate change, and environmental issues such as ozone formation, acid deposition, and smog [6]. Long-term exposure to certain VOCs can also present serious health risks, including cancer [7].

In light of current conditions, maintaining air quality has become essential for public health and the long-term well-being of humanity. One of the most widely used methods for air purification is particulate filtration, which works by capturing airborne particles through filters made from membranes, fibrous or porous materials [8]. However, filters can accumulate microbes, allowing bacteria to grow, and becoming a vehicle of infection. To address this, antibacterial filters are

* Correspondence to: Department of Applied Science and Technology, Politecnico di Torino, Torino (TO), Italy, Institute of Materials Engineering and Physics, Corso Duca degli Abruzzi, 24, 10129 Torino, Italy.
E-mail address: marta.miola@polito.it (M. Miola).

https://doi.org/10.1016/j.materresbull.2026.114305
Received 17 April 2026; Received in revised form 15 June 2026; Accepted 19 June 2026
Available online 20 June 2026

recommended to prevent bacterial growth [9].

Materials such as activated carbon, zeolite clay, silica gel, activated alumina, mineral clay, and certain polymers have demonstrated the ability for surface sorption. The highly ordered pore structure at the molecular level permits only molecules of specific sizes to enter certain pores. Zeolite, in particular, has shown a strong capacity to adsorb volatile organic compounds (VOCs) like toluene, methanol, and benzaldehyde, making it a promising adsorbent for improving indoor air quality [10]. However, one disadvantage concerning the adsorption-based purification methods is that they only transfer the pollutant from the gas phase to the surface of a solid and therefore offer a temporary solution. Conversely, catalytic oxidation provides a permanent removal pathway by converting harmful molecules into innocuous products such as CO_2 and H_2O. For this reason, catalysis represents a more effective and sustainable strategy for indoor air purification. Moreover, another disadvantage of the use of synthetic zeolites is the high cost of production. To overcome this fact, in recent years, natural zeolites have gained considerable interest because of their unique chemical and physical characteristics, as well as their cost-effectiveness, since they are produced through natural processes, making them a suitable alternative to synthetic zeolites [11]. Among them, Clinoptilolite is regarded as the most common and abundant natural zeolite, with numerous studies demonstrating its effectiveness in removing pollutants from gas streams, including carbon dioxide, methane, and ammonia [12]. However, it lacks antibacterial activity [13,14] and does not exhibit catalytic properties in its natural form [15], but it can be easily modified for these purposes; in fact, the aluminosilicate framework of clinoptilolite serves as an ion-exchange medium, allowing it to host various metallic ions [16]. This property is crucial for its modification, particularly in the incorporation of nanoparticles [17].

Among antibacterial agents, silver ions have long been recognized for their potent inhibitory and bactericidal effects, as well as their broad-spectrum antimicrobial activity [18,19]. It is now widely accepted that the antibacterial actions of silver nanoparticles (AgNPs) involve not only the damage to intracellular biomolecules and structures, as well as oxidative stress caused by the released silver ions, but also their attachment to the cell wall and membrane, along with damage to intracellular components caused by AgNPs themselves [20]. Moreover, they have also demonstrated activity against viruses as well [21].

The literature provides numerous examples of introducing silver into clinoptilolite through ion exchange [13,22,23], including for antibacterial purposes in the filtration field. Additionally, silver nanoparticles have been synthesized and supported on clinoptilolite using ion exchange followed by heat treatments [24,25] or through absorption methods [26].

In contrast, few studies in the literature focus on the use of natural zeolites for catalytic oxidation. Clinoptilolite is typically employed to form composites by adding TiO_2 [27] or as a support for palladium-copper complexes [28] and other noble metals, often used for the removal of toluene, although these additions increase costs. However, there is limited information on its application in the catalytic oxidation of common indoor pollutants. Among these, CO and VOCs (such as ethylene) pose significant health risks and are frequently found in enclosed, confined spaces. They can originate from incomplete combustion during cooking or from cigarette smoke, and are known to provoke significant negative effects on human health [29]. CO is one of the most common and critical indoor contaminants, generated by incomplete combustion from gas heaters, cooking appliances, fireplaces, tobacco smoke, and even infiltration from attached garages; it is highly toxic even at low concentrations, making its complete oxidation a priority for indoor air purification [30,31]. Ethylene, on the other hand, was chosen as a simple model compound for unsaturated VOCs, representative of hydrocarbon emissions. Although less immediately toxic than CO, ethylene is widely present indoors due to emissions from cooking (thermal decomposition of organic matter and oils), off-gassing from plastics and building materials, and plant metabolism or fruit-ripening processes [32]. Even trace levels of ethylene (ppb-ppm) can accelerate the deterioration of fresh products during storage and have been associated with respiratory irritation, asthma, and allergic responses [32–34]. Based on these premises, the removal of these molecules from indoor spaces is urgent. While silver nanoparticles have been investigated for catalytic purposes [35,36], the use of Ag-functionalized clinoptilolite in this area remains underexplored.

However, the development of multifunctional natural zeolite-based materials combining catalytic oxidation of gaseous pollutants with antibacterial activity remains scarcely explored, particularly when green functionalization routes are employed. The primary goal of this work is to evaluate the effectiveness of Ag-containing clinoptilolite in removing both biological and gaseous contaminants, positioning it as a viable and cost-effective alternative for air purification systems. Silver is introduced in two forms—ionic and metallic—to explore its specific role in contaminant removal.

2. Materials and methods

2.1. Materials

Natural zeolite clinoptilolite came from a deposit in England and was provided by Heiltropfen Lab. LLP company. Tannic Acid (TA, ACS reagent grade) was used as a reducing agent for the green reduction in situ of the silver nanoparticles (AgNPs) and silver nitrate ($AgNO_3$, 99%, Sigma Aldrich) was used as the silver source in the process. Potassium carbonate (K_2CO_3, 99%, Sigma Aldrich) and sodium hydroxide (NaOH, >98%, Sigma Aldrich) were used to maintain an alkaline pH during the process. All reactants were purchased by Merck (Darmstadt, Germany).

2.2. Functionalization with Ag through ion exchange

For silver functionalization via ion exchange, natural clinoptilolite was soaked in a 0.5 M aqueous solution of silver nitrate ($AgNO_3$) for three hours in the ratio 30 mg/mL to enable the ion exchange process. The resulting Clino-Ag powders were centrifuged at 12,000 rpm for 10 min to separate the zeolite from the solution, then rinsed with deionized water two times and dried overnight at 70°C.

2.3. Functionalization with AgNPs

The functionalization with silver nanoparticles was carried out as described in a previous work by the authors [14]. Clinoptilolite was first functionalized with tannic acid, which acted as a reducing agent for the in situ reduction of silver nanoparticles. The resulting Clino-TA was then immersed in a 0.5 M aqueous solution of silver nitrate ($AgNO_3$) for three hours in the same ratio of 30 mg/mL. The concentration of silver precursor was kept consistent with that used in the ion exchange process to evaluate the effect of tannic acid in the silver introduction process. After this, the Clino-AgNPs were isolated by centrifugation at 12,000 rpm for 10 min two times and dried overnight at 70°C, as previously reported. Fig. 1 illustrates the two functionalization processes.

2.4. Sample characterization

2.4.1. Physicochemical characterization

Clino-AgNPs was already characterized in the authors' previous work [14]. The sample Clino-Ag was characterized morphologically through Field-Emission Electron Microscopy (FESEM-EDS SUPRATM 40, Zeiss and Merlin Gemini Zeiss), equipped with Energy Dispersive X-ray Spectrometry (FESEM-EDS SUPRATM 40, Zeiss and Merlin Gemini Zeiss and MIRA3 XMH, TESCAN). The distribution of the silver on the samples was detected through elemental maps obtained with high-resolution scanning transmission electron microscopy (STEM, Talos Thermo Scientific) with a LaB6 gun, operating at 200 kV.

The characterization in terms of the sample structure was performed

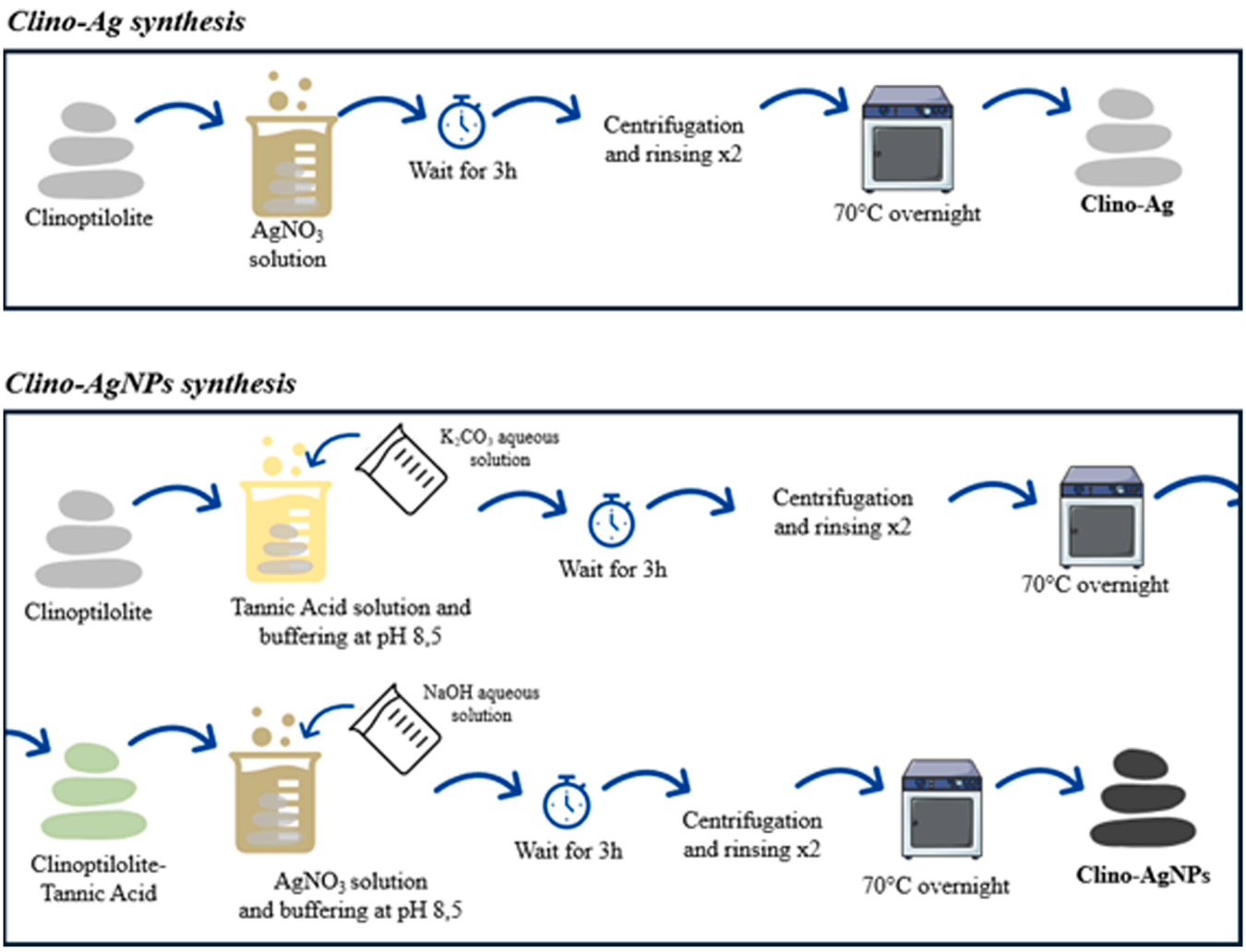

Fig. 1. Scheme of silver-functionalization processes of Clinoptilolite. The Figure was drawn in part using images from Servier Medical Art. Servier Medical Art by Servier is licensed under a Creative Commons Attribution 3.0 Unported License (https://creativecommons.org/licenses/by/3.0/).

using X-ray diffractometry (XRD, Bragg–Brentano X′pert Philips diffractometer) using the Bragg Brentano camera geometry and the Cu-Ka incident radiation. The 2θ range used for sample measurements was from 30° to 90° in order to check that the silver was introduced only in the ionic form in the sample.

2.4.2. *Textural properties*

Textural properties were determined by N_2 and CO_2 adsorption at 77 and 273 K, respectively (Micrometrics ASAP 2020Plus). Before the measurement, the samples were outgassed under vacuum at 423 K for 3 h. From the N_2 adsorption isotherms, the specific surface area (SSA) of the samples was calculated according to the BET (Brunauer–Emmet–-Teller) method. Micropore volume, V_{MP}, was calculated by applying the *t*-plot method. For carbon dioxide isotherm, the specific surface area and total pore volume have been calculated by applying the Dubinin-Radushkevich (DR) and the Langmuir model.

2.4.3. *Catalytic performance*

Catalytic oxidation experiments were conducted in a fixed-bed quartz U-shaped reactor (ID = 4 mm) heated by a PID-controlled furnace. The temperature of the bed was measured using a K-type thermocouple inserted into the reactor. Prior to starting the reaction, 50 mg of powder catalyst was pretreated under a 100 $mLmin^{-1}$ flow of pure N_2 at 150 °C for 1 h to remove physisorbed species (such as moisture and other gaseous compounds). After natural cooling to room temperature, a gaseous reactive mixture, simulating a real indoor environment, was introduced into the reactor at a flow rate of 50 $mLmin^{-1}$. The mixture consisted of the maximum concentration of a gaseous pollutant typically found in confined spaces (100 ppm of pollutant, which could be CO or ethylene chosen as probe molecules), 21 vol% O_2, and the remainder N_2. During the test, the catalyst weight-to-volumetric flow rate ratio (W/F) was 0.017 ghL^{-1}. The experiment started at 25 °C, with the temperature gradually increased in isothermal steps of 25 °C increments to avoid the effects of adsorption-desorption phenomena. The test concluded when the pollutant conversion reached 100% or it was stopped at the maximum temperature of 250 °C. The composition of the outlet gas was continuously monitored using a non-dispersive infrared (NDIR) gas analyzer (ABB Uras 14, ABB S.p.A – PAMA, Milan, Italy) connected to the reactor outlet. For comparison, a bare clino sample was also tested. Finally, to better investigate the stability of the best-performing catalyst, a time-on-stream (TOS) analysis was conducted on the same apparatus. Specifically, 50 mg of the sample was placed in the reactor by feeding the polluted air containing 100 ppm of pollutant. The temperature was fixed at the value at which the conversion reached 90% for CO and 50% for ethylene oxidation and it was kept constant for 8 h in order to evaluate the stability of the catalyst under continuous flow.

2.4.4. *Antibacterial activity evaluation – bioaerosol contamination*

For the antibacterial testing, pellets of Clino, Clino-AgNPs, and Clino-

Ag were prepared; the samples were exposed to a bacterial bioaerosol, using an experimental setup developed by Balagna et al. [37] which involved a compressed air system and a bioaerosol generator (TOPAS ATM 220). A bacterial aerosol was generated from standardized suspensions of non-pathogenic strains of *Staphylococcus epidermidis* (Gram-positive, ATCC14990) and *Escherichia coli* (Gram-negative, ATCC8739) colonies (McFarland index 5.0) and nebulized onto the pellets at an airflow of 3 bar. After contamination, the samples were transferred to Mueller–Hinton agar plates (for *S. epidermidis*) and Nutrient agar plates (for *E. coli*) and incubated at 35 °C for 24 and 48 h. Bacterial growth around and underneath the sample surface was then evaluated. The antibacterial test was also performed on the zeolites previously used in the catalytic experiments, to assess whether their antibacterial activity was retained after exposure to the oxidation reaction conditions.

3. Results and discussion

3.1. Physiochemical characterization

FESEM images of the Clino samples are shown in Fig. 2. The typical lamellar structure of this natural zeolite is clearly visible in Fig. 2(a,b) [38], along with the effects of cleavage [39]. The appearance of the exchanged zeolite is very similar to the unfunctionalized form, with no observable changes in grain morphology (Fig. 2c,d) [14]. An increase of the dispersion of the zeolite grains can be associated with the ion exchange process during which clay minerals are removed [40]. No nanoparticles are visible on the surface, in contrast to the Clino-AgNPs sample from previous work [14], which displayed small particles on the grain surface (Fig. 2e,f).

STEM imaging was performed to achieve higher magnifications and examine the morphology of the zeolite grains following the two functionalization processes. STEM is an effective technique for analyzing supported nanoparticles, as small metal or alloy nanoparticles on high surface-area supports are easily detected in STEM images [41]. As shown in Fig. 3a and b, the Clino-AgNPs sample displays small, well-distributed nanoparticles across the surface in both dark field and bright field images; the contrast between the zeolite matrix and the supported AgNPs is clear. In the Clino-Ag sample (Figs. 3c and 3d) only a few nanoparticles are visible on the surface, likely due to the heating effect of the electron beam, a known phenomenon in nanoparticle research also used to study the in situ sintering of metallic systems [42]. For zeolites exchanged with metal ions, the reduction of the ions to their metallic state can occur during STEM/TEM analysis, as the electron beam, under vacuum conditions, locally heats the samples. This localized heating can lead to the formation of reduced silver species, such as clusters or metallic nanoparticles [43].

To further assess the spatial distribution and speciation of silver on clinoptilolite, STEM–EDS elemental mapping was carried out on the same particles shown in Fig. 3. The resulting Si, Al, and Ag elemental maps are reported in Fig. 4. Silicon and aluminium signals are uniformly distributed throughout the zeolite crystals, confirming the homogeneous composition of the framework. In contrast, the Ag maps clearly reveal two distinct distributions depending on the synthesis route. In Clino-

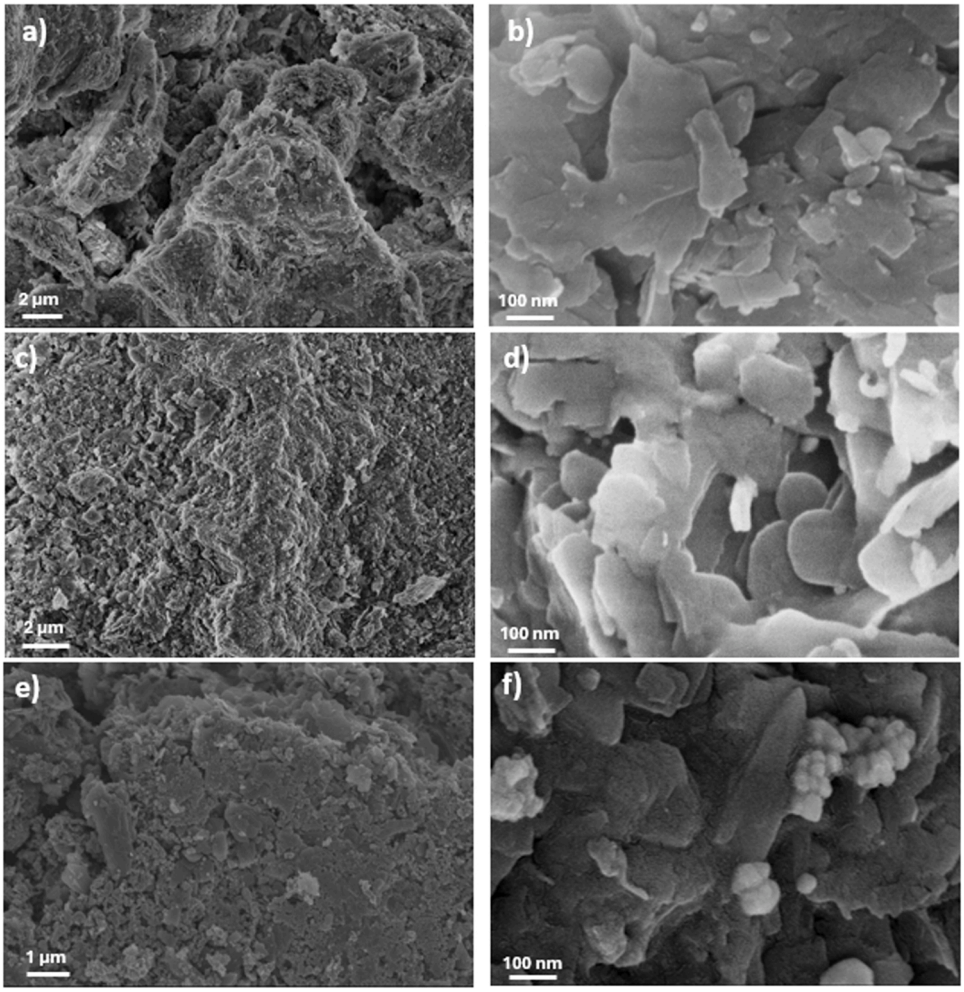

Fig. 2. FESEM images of the sample Clino (a,b), Clino-Ag (c,d) and Clino-AgNPs (e,f).

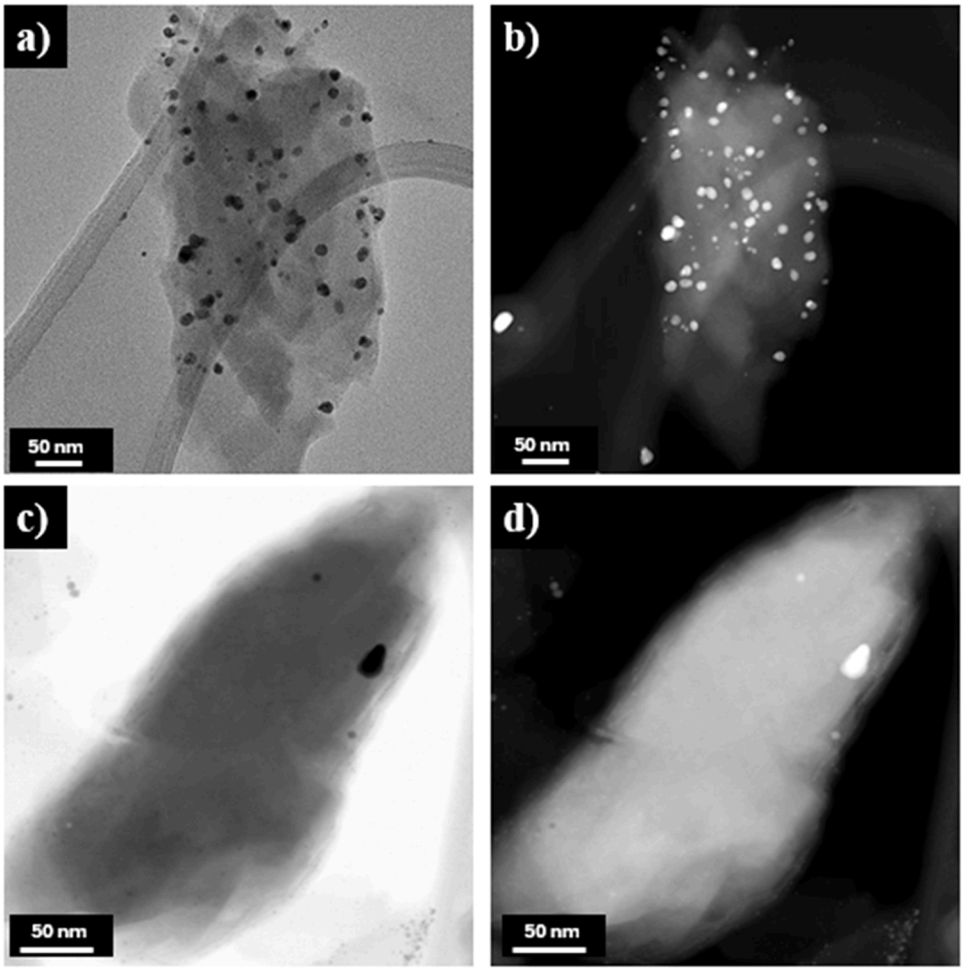

Fig. 3. STEM images of Clino-AgNPs (a,b) and Clino-Ag (c,d) in bright field (a,c) and dark field (b,d).

AgNPs (Fig. 4c), silver appears as discrete and well-defined nanosized spots, consistent with the presence of metallic Ag nanoparticles anchored on the external surface. In Clino-Ag (Fig. 4f), the Ag signal is instead diffuse and lacks defined clusters (except for an isolated bright spot, likely associated with beam-induced reduction during STEM acquisition), indicating that silver is predominantly present in an ion-exchanged state within the zeolite framework rather than as segregated nanoparticles. These results confirm that tannic-acid reduction promotes the formation of surface-exposed AgNPs, whereas ion exchange mainly leads to dispersed ionic silver within the clinoptilolite structure.

EDS analysis was performed on the Clino-Ag and Clino-AgNPs samples to quantify the silver introduced into the zeolite via two eco-friendly functionalization methods. As shown in Table 1, the main components of clinoptilolite are oxygen, aluminum, and silicon, with small amounts of sodium, potassium, and calcium. The levels of these exchangeable metals, which can be replaced by silver [38], decreased after silver functionalization and remained comparable between the two methods, indicating that ion exchange occurred in both samples. The key difference was the silver content: clinoptilolite after the in-situ reduction resulted in three times higher silver content compared to simple ion exchange, highlighting a significant role of tannic acid in introducing a higher amount and different form of silver on the surface of the Clino starting from the same initial silver precursor concentration.

XRD structural analysis, reported in Fig. 5, confirmed the absence of metallic silver in the Clino-Ag sample. The pattern obtained for Clino-Ag when compared to that of Clino-AgNPs, shows no indication of metallic silver formation; in fact, the characteristic peaks of metallic silver located at 38.1°, 44.3°, 64.4°, 77.5° (JCPDS card of Ag (NO. 04–0783) [44]) are only present in the sample Clino-AgNPs. The peaks detected in the patterns of Clino and Clino-Ag are mainly related to the highly crystalline structure of natural zeolite clinoptilolite [45]. This analysis was essential for accurately comparing the activity of ionic versus metallic silver in the application of these zeolites for air decontamination. To verify the stability of the silver species during operation, XRD analyses were performed on both Clino-Ag and Clino-AgNPs after the catalytic tests. The diffraction patterns (Fig. 5b) show the same phase composition observed in the fresh powders, with no appearance of new reflections or peak shifts. In particular, the characteristic reflections of metallic Ag (2θ = 38.1°, 44.3°, 64.4°, 77.5°) remain unchanged in Clino-AgNPs, and no metallic silver peaks appear in Clino-Ag. These results confirm that the silver speciation (ionic vs. metallic) and the crystallographic phases remain stable during catalysis.

3.2. *Textural properties*

The effect of the different Ag functionalization procedures on textural properties was investigated by means of N_2 and CO_2 adsorption at 77 and 273 K, respectively. For natural clinoptilolite, low-temperature N_2 adsorption is not fully suitable for probing microporosity, as the very small channel apertures of the HEU zeotype framework lead to diffusion limitations and consequent underestimation of the microporous volume. Accordingly, bare Clino exhibited a type II N_2 isotherm (Figure SI−1 and table SI−1), which is generally associated with non-porous (or macroporous) materials [46]. The H3-type hysteresis loop can be attributed to capillary condensation in inter-particle

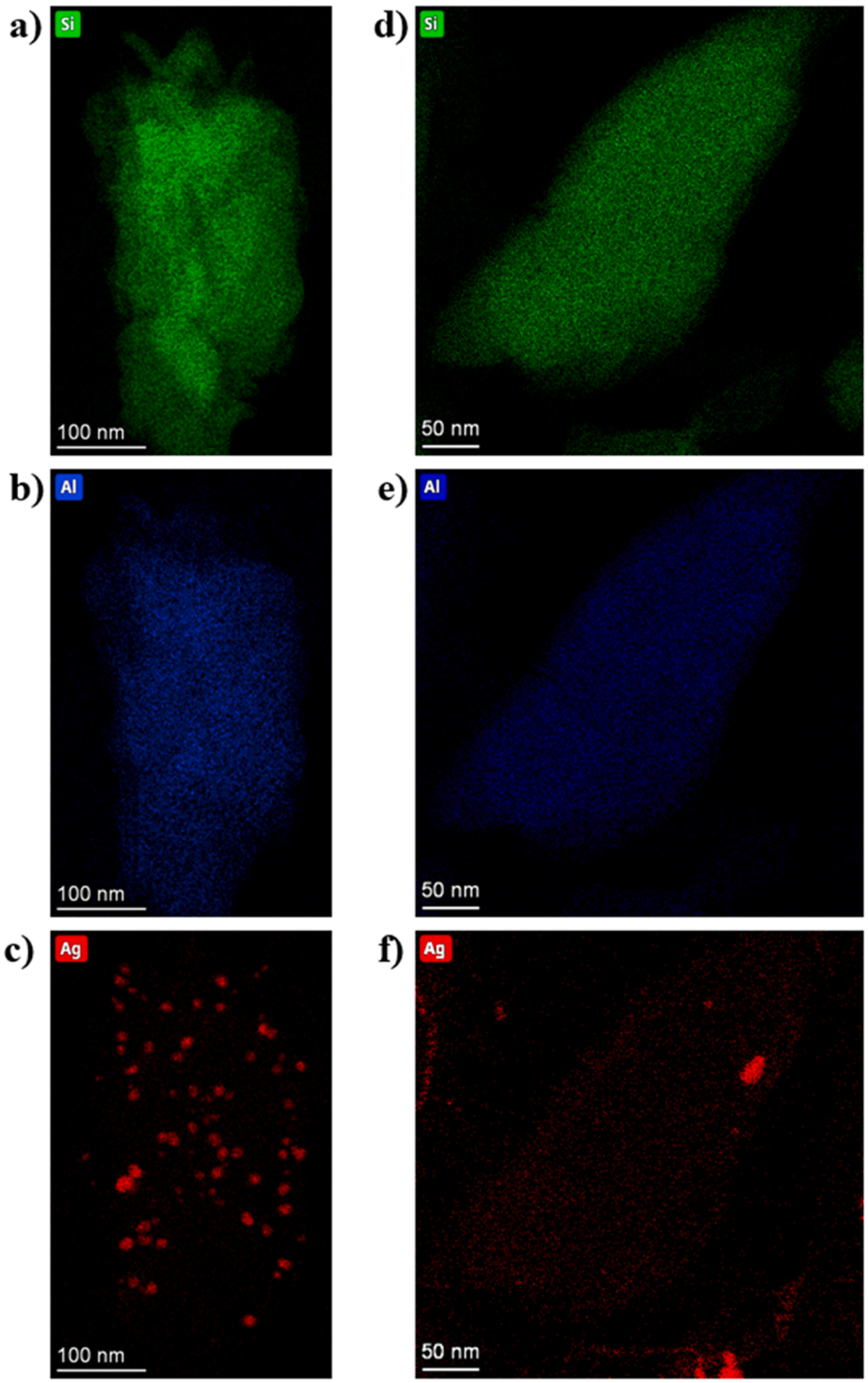

Fig. 4. STEM–EDS elemental maps of Si (green), Al (blue), and Ag (red) for Clino-AgNPs (a–c) and Clino-Ag (d–f).

large mesoporosity, whereas the limited increase in adsorbed N_2 volume at very low relative pressures indicates a very small microporous volume ($V_{MP} = 2{\cdot}10^{-3}$ cm^3g^{-1}). Therefore, it is likely that the SSA measured by N_2 (30 m^2g^{-1}) corresponds predominantly to the external surface area of the particles. Similar features are commonly found in the literature for clinoptilolite samples [47–49] and were also observed for Clino-AgNPs, where the addition of a much heavier element contributes to the decrease in SSA (21 m^2g^{-1}). According to previous studies, the limitations of using N_2 as a probe molecule to determine the actual textural properties were overcome by employing CO_2 adsorption measurements at 273 K, since it is well known that at this temperature CO_2 does not encounter diffusion limitations within the narrower micropores [50,51]. In contrast to the N_2 isotherm, the CO_2 isotherm of all the samples (Fig. 6) is of type I, as expected for a microporous material. Both the Langmuir and DR models [52] yielded SSA values significantly higher than those obtained from nitrogen measurements (e.g. SSA_{Lang} =

Table 1
Elemental composition of Clino, Clino-Ag and Clino-AgNPs.

Sample		O	Na	Al	Si	K	Ca	Ag
Clino	% At.	64.4±0.1	0.6±0.1	4.7±0.1	27.6±0.1	1.7±0.1	1±0.2	-
	% Weight	50.3±0.2	0.8±0.1	6.3±0.2	37.8±0.2	3±0.3	1.9±0.5	-
Clino-Ag	% At.	70.9 ±2.2	0.14±0.2	4.1±0.5	21.5±1.6	0.8±0.2	0.4±0.2	**2.3±0.4**
	% Weight	53.2 ±3.2	0.16±0.2	5.2±0.5	28.2±1.5	1.4±0.3	0.8±0.3	**11.1±1.2**
Clino-AgNPs	% At.	61.5 ±0.4	0.14±0.1	4.2±0.1	25.4±0.3	1.1±0.1	0.2±0.1	**7.6±0.4**
	% Weight	36.8 ±0.9	0.11±0.1	4.2±0.1	26.6±0.9	1.7±0.2	0.2±0.2	**30.4±1.8**

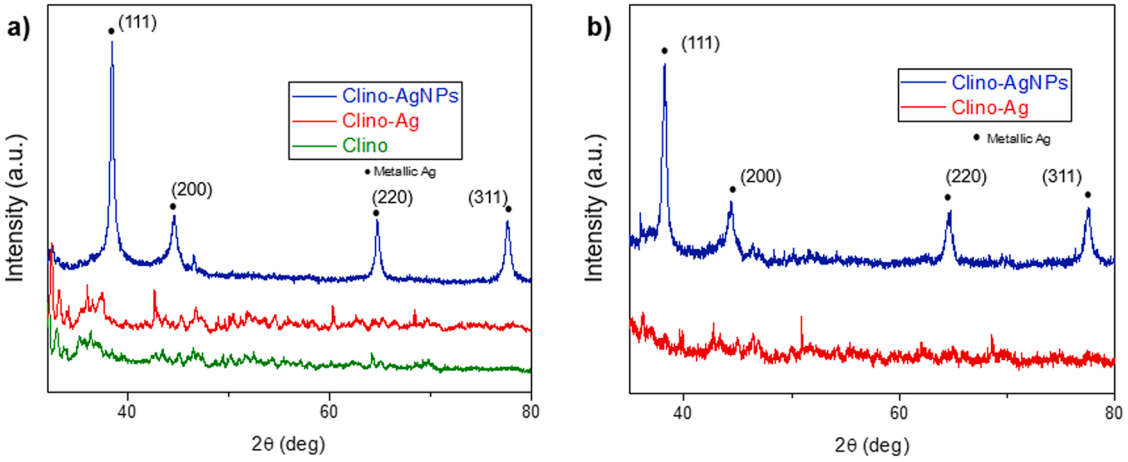

Fig. 5. XRD pattern of Clino, Clino-Ag, Clino-AgNPs before (a) and after catalytic tests (b).

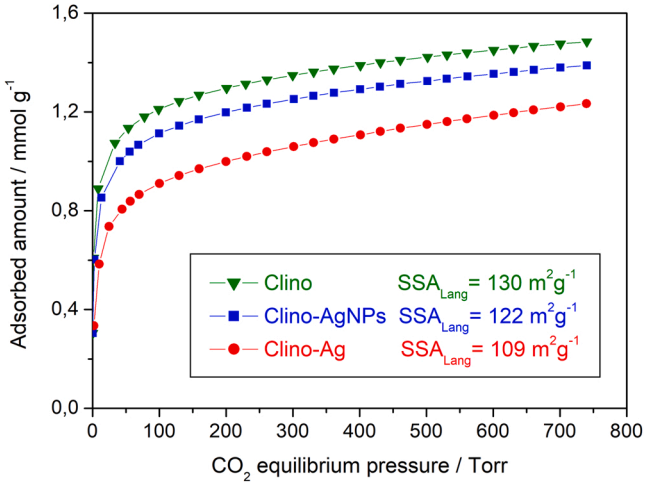

Fig. 6. CO_2 Adsorption isotherm at 273 K of Clino, Clino-AgNPs and Clino-Ag.

130, 122 and 109 m^2g^{-1} for Clino, Clino-AgNPs and Clino-Ag, respectively). Interestingly, despite its lower Ag content, sample Clino-Ag exhibited SSA and V_{MP} (DR) slightly lower than Clino-AgNPs, likely due to the location of some Ag^+ ions close to the smaller 8-member ring apertures of the HEU-zeotype framework, thereby reducing the effective internal surface probed by CO_2. This effect is moderate and does not imply full pore blockage, but simply a reduced micropore surface available to the probe molecule. The different nature of Ag in the two samples is also evidenced by the comparison of K (Langmuir constant) and E_o (characteristic Energy of the DR model), which are similar for Clino and Clino-AgNPs, but lower for Clino-Ag (Figure SI−2). Both constants depend on the CO_2-adsorbate interaction strength, and their decrease agrees with the lower polarizing power (due to the larger ionic radius) of Ag^+ compared to that of Na^+, with which Ag^+ is likely exchanged. Overall, the CO_2 adsorption measurements do not show significant pore-blocking effects and confirm the actual ion exchange for the Clino-Ag sample.

3.3. Catalytic activity evaluation

The catalytic activity results are summarized in Fig. 7. All catalytic experiments were performed in triplicate, and the corresponding error bands shown in Fig. 7 demonstrate the good reproducibility of the catalytic performance for all investigated samples. Overall, Clino-AgNPs demonstrated remarkable performance, completely oxidizing CO below 125 °C, that is a significant improvement compared to both Clino-Ag and bare Clino samples. When comparing the results with the bare Clino, it was evident that this sample only reached about 60% conversion at 250 °C, while Clino-Ag achieves approximately 80% conversion at the same temperature, highlighting the enhanced performance of both silver-modified samples. In the case of ethylene, a more challenging molecule to oxidize due to the presence of a C═C double bond, a similar trend was observed. Clino-AgNPs exhibited superior catalytic activity, achieving over 60% conversion at 250 °C, which was substantially higher than the conversion achieved by both Clino and Clino-Ag, which remained well below 10% conversion at the same temperature. This substantial improvement emphasizes the key role played by the presence of silver nanoparticles on the surface of Clino-AgNPs in enhancing catalytic performance. Moreover, as reported in Table SI−2, by evaluating the conversion rates normalized per mass of silver, it was evident that Clino-AgNPs exhibited significantly higher reaction rates for both CO (318.4 vs 141.9 μmol h^{-1} g_{Ag}^{-1}) and ethylene oxidation (213.0 vs 71.3 μmol h^{-1} g_{Ag}^{-1}) compared to the ion-exchanged Clino-Ag sample. These results clearly demonstrate that metallic Ag nanoparticles provide a substantial enhancement in intrinsic catalytic activity compared to exchanged Ag species, highlighting the superior efficiency of surface Ag^0 sites in promoting oxidation reactions. Thus, for both the pollutants tested, the addition of AgNPs to the zeolite surface significantly boosted catalytic performance. By comparing the two silver-containing samples, it appears that the presence of Ag^+ ions mostly in the zeolite framework

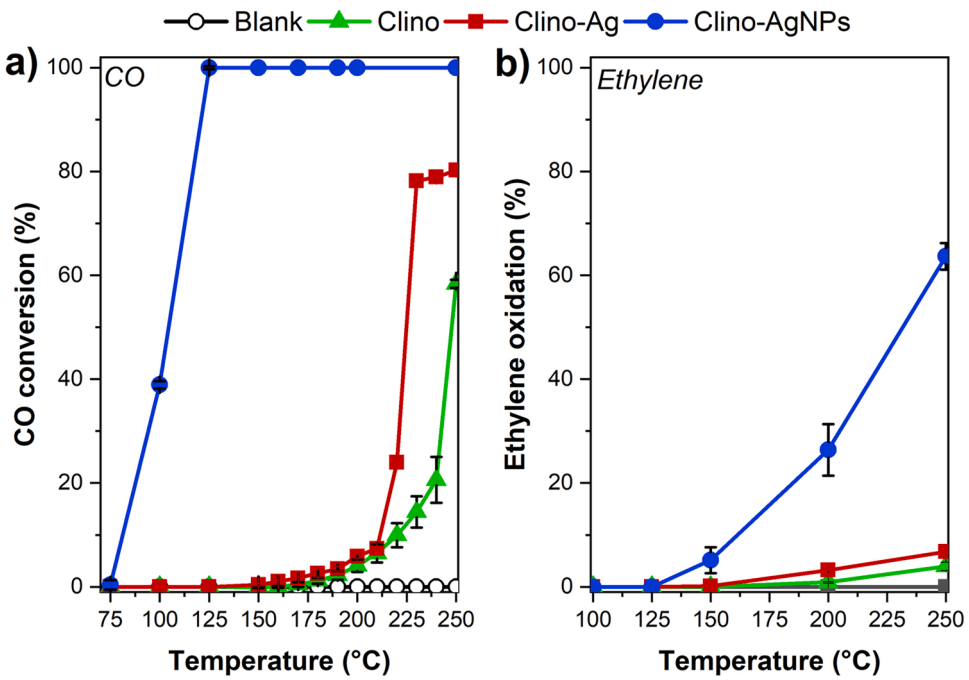

Fig. 7. Catalytic conversion of CO (a) and ethylene (b) as a function of the temperature in dry conditions, feeding gaseous mixture with 100 ppm of pollutant, 21 vol % O_2 and N_2 to balance over 50 mg of catalyst.

is insufficient to efficiently oxidize the pollutants. According to existing literature [53,54], the concurrent presence of both Ag^+ and Ag^0 species has been shown to positively influence catalytic activity, suggesting that the silver nanoparticles may be playing a critical role in facilitating the oxidation process.

The different catalytic trends observed for CO and ethylene oxidation can be explained by considering differences in terms of size, diffusion, and reaction mechanism between the two reactant molecules. CO, due to its small kinetic diameter, can readily diffuse into the clinoptilolite channels. Although Ag^+ is catalytically active toward CO oxidation, as revealed from catalytic tests, its activity is significantly lower than that of metallic Ag nanoparticles, indicating that Ag^0 is more effective in activating CO. In contrast, ethylene oxidation is strongly limited by steric and diffusional constraints. The larger kinetic diameter of ethylene hinders its diffusion into the narrow pores of clinoptilolite, resulting in poor performance even for the bare zeolite without silver. Therefore, the low activity observed for ethylene may reflect an intrinsic diffusion limitation within the zeolite framework. Moreover, ethylene oxidation requires different active sites and adsorption geometries compared to CO, making surface-exposed metallic Ag nanoparticles particularly advantageous, while exchanged Ag^+ species inside the pores are largely inaccessible and, in turn, ineffective. As a result, diffusion limitations dominate ethylene oxidation, whereas for CO oxidation, both diffusion and the nature of the Ag active site contribute, explaining why AgNPs show a pronounced advantage for CO but only a moderate improvement for ethylene.

In silver-containing zeolite systems, the chemical form and localization of Ag were found to be crucial for catalytic activity. In particular, the literature showed that metallic Ag NPs were responsible for both catalytic and antibacterial activity [55,56]. Conversely, ion-exchanged Ag^+ species exhibited very low activity [56,57]. This was consistent with the results presented in this work. In fact, surface-exposed nanoparticles allowed both oxygen and the pollutant to adsorb, react, and desorb the products. In contrast, Ag^+ within the micropores of the zeolite showed strongly limited steric accessibility for O_2 and pollutants, thereby reducing the molecules-oxygen-Ag contact and catalytic activity.

When comparing the results obtained in this work with the existing literature (see table SI−3), it is clear that the catalytic performances of Clino-AgNPs are either equal or even superior to those reported in other studies. It is worth noting that relatively few studies have investigated the use of natural zeolitic materials in catalytic applications. For example, Bagnasco et al. [58] reported a total ethylene conversion of approximately 50% when using a natural zeolite (chabazite) in combination with silver (Ag). The results were comparable to the catalytic performance achieved in the present study. In contrast, López-Hernández et al. [59] reported a total CO conversion at a significantly higher temperature of 400 °C, which exceeds the temperature conditions tested in this work. These examples demonstrate the effectiveness of natural zeolitic materials obtained through green synthesis and highlight the promising catalytic performance of these materials in various applications.

To better investigate the performance and the stability of the best-performing catalyst Clino-AgNPs, time-on-stream (TOS) analysis was carried out for 8 h under continuous reaction conditions. The results were reported in Fig. 8. As can be seen, in the case of CO oxidation, the catalyst exhibited an exceptionally stable behavior, maintaining a remarkably high and constant CO conversion of 91.7 ± 0.3%, with no observable deactivation throughout the 8-hour CO oxidation experiment. Conversely, ethylene oxidation showed a more dynamic response, with the conversion initially fluctuating before stabilizing around 29.4 ± 7.9%. This behavior may be attributed to the slower oxidation kinetics of ethylene and to the different balance between the rate at which active sites are freed after reaction and the rate at which the pollutant molecules arrive at the surface. Such a mismatch can lead to a gradual decline in the availability of active sites under steady-state conditions, ultimately resulting in the observed decrease in conversion over time. Overall, the TOS profiles clearly demonstrated that the Clino-AgNPs catalyst possessed good operational stability, especially in CO oxidation, where its performance remained essentially unchanged throughout the 8 h test. These results indicate promising short-term durability under continuous operation and support the potential application of the material in air purification systems. However, catalyst recyclability through repeated reaction-regeneration cycles and longer-term stability tests can be addressed in future studies to evaluate possible Ag nanoparticle sintering, silver leaching, or catalyst deactivation during extended

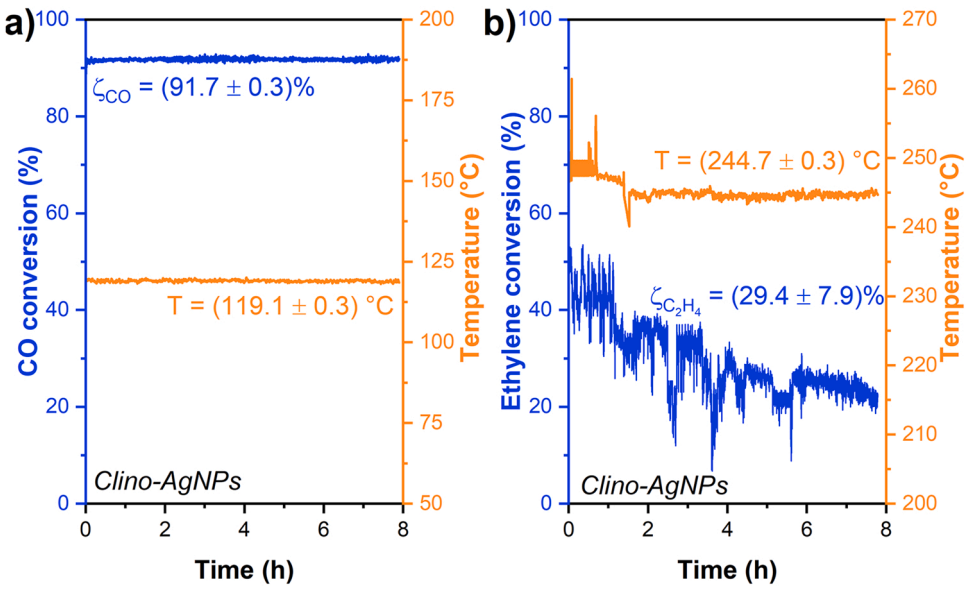

Fig. 8. Time-on-stream (TOS) analysis performed at isothermal conditions by feeding polluted air with 100 ppm of CO (a), and ethylene (b) over 50 mg of Clino-AgNPs catalyst.

operation.

Although no definitive mechanism has been experimentally established for these pollutants on Ag-zeolite catalysts, several studies on silver nanoparticles and Ag nanoclusters provided insights that allow proposing a plausible pathway [60,61]. For instance, DFT studies on Ag nanoclusters (Ag_{55}) showed that both CO and O_2 can adsorb on metallic silver sites and that CO oxidation can proceed through a co-adsorption mechanism, where O_2 is activated on the Ag surface and subsequently reacts with adsorbed CO to form CO_2 [62]. Similar conclusions were reached for small Ag-Au clusters, where a co-adsorption pathway displayed the lowest activation barriers for CO oxidation [60].

3.4. *Antibacterial activity evaluation – Bioaerosol contamination*

The standardized bacterial suspensions of *S. epidermidis* and *E. coli* were nebulized onto Clino, Clino-Ag, and Clino-AgNPs pellets for 30 min. Following contamination, the pellets were incubated on Muller Hinton and Nutrient agar plates, and the results are displayed in Fig. 9. Bacterial growth was assessed after 24 and 48 h of incubation. As shown in Figs. 9a and 9c, pure clinoptilolite does not inhibit bacterial proliferation, with clear colony formation observed after 24 h of incubation time. In contrast, both Ag-containing samples (Clino-Ag and Clino-AgNPs) exhibit a complete suppression of bacterial growth for both Gram-positive and Gram-negative strains; this indicates that bacteria sprayed onto the surface of the Clino-Ag and Clino-AgNPs pellets were completely eradicated. Both silver ions and silver nanoparticles are well-established antibacterial agents [63]. Ionic silver (Ag^+) disrupts essential cellular functions through interactions with proteins, enzymes, and nucleic acids, while silver nanoparticles (AgNPs), through direct contact with bacterial cells, can induce membrane damage and oxidative stress

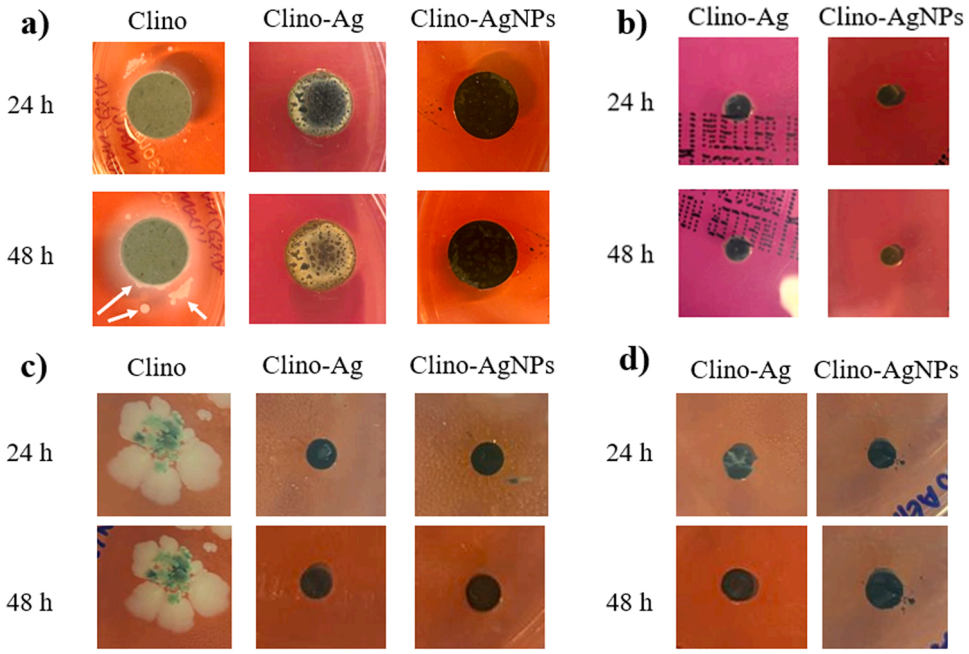

Fig. 9. Bioaerosol contamination test with *S. epidermidis* (a,b) and *E. Coli* (c,d) on Clino, Clino-Ag, Clino-AgNPs before (a,c)) and after catalytic tests (b,d).

[64]. In gas-phase antibacterial tests based on bioaerosol exposure, direct contact between bacteria and the material surface represents the dominant inactivation mechanism, making surface-exposed AgNPs particularly effective for this type of application. Nevertheless, the ion-exchanged Clino-Ag sample also exhibits a clear antibacterial effect. This behavior can be attributed to the presence of Ag^+ species located at or near the external surface, which are sufficient to exert antibacterial activity, as well as to the experimental conditions employed. In particular, local humidity and contact with the agar medium may promote partial Ag^+ release from near-surface exchange sites, contributing to bacterial inactivation even in the absence of metallic nanoparticles.

The test was repeated on the samples recovered from the experiments with CO and ethylene to check if the antibacterial activity was preserved after oxidation reaction. As shown in Fig. (9b,d), the small pellets made from the powders used in the catalytic tests show no bacterial colony formation after 24 and 48 h of incubation, suggesting a potential application against both bacteria and contaminants at the same time. When AgNPs are supported, they do not undergo aggregation during catalytic activities, allowing them to retain their antibacterial properties [65].

4. Conclusions

Clinoptilolite was successfully functionalized using eco-friendly methods, yielding two samples with silver in distinct forms: metallic and ionic. The resulting samples, Clino-AgNPs and Clino-Ag, displayed different morphologies and structures, confirming variations in both silver content (starting from the same concentration of silver precursors) and form. The presence of metallic silver nanoparticles led to improved textural properties and significantly enhanced clinoptilolite's performance in contaminant removal. Notably, the excellent textural properties of natural clinoptilolite were maintained, and the catalytic performance toward CO and ethylene increased with the introduction of silver nanoparticles. In contrast, no such improvement was observed with silver ions. Nevertheless, both forms of silver exhibited excellent antibacterial properties against both Gram-positive and Gram-negative strains, irrespective of their structural differences. Although tannic acid-assisted in situ reduction is expected to favour AgNP immobilization on clinoptilolite compared with simple surface adsorption, the possible release of silver nanoparticles under realistic air-flow conditions could not be quantitatively assessed in the present study, also due to the lack of standardized methods specifically addressing nanoparticle release. This aspect should be further investigated for practical filtration applications.

Overall, these findings highlight the potential of silver-functionalized clinoptilolite, particularly Clino-AgNPs, as a highly effective material for air purification, combining enhanced contaminant removal with strong antibacterial properties, making it a promising candidate for environmental and public health protection.

CRediT authorship contribution statement

Marco Piumetti: Writing – review & editing, Writing – original draft, Conceptualization. **Marta Miola:** Writing – review & editing, Writing – original draft, Supervision, Resources, Project administration, Methodology, Investigation, Funding acquisition, Conceptualization. **Francesca Gattucci:** Writing – review & editing, Writing – original draft, Visualization, Investigation. **Mari Sofia Lallukka:** Writing – review & editing, Writing – original draft, Visualization, Investigation. **Nadia Grifasi:** Writing – review & editing, Writing – original draft, Visualization, Investigation. **Marco Armandi:** Writing – review & editing, Writing – original draft, Visualization, Investigation.

Declaration of Generative AI and AI-assisted technologies in the writing process

During the preparation of this work, the authors used ChatGPT in order to improve the readability of the paper and to check the language errors. After using this tool, the authors reviewed and edited the content as needed and take full responsibility for the content of the publication.

Declaration of Competing Interest

The authors declare that they have no known competing financial interests or personal relationships that could have appeared to influence the work reported in this paper.

Acknowledgments

This study was carried out within the MICS (Made in Italy – Circular and Sustainable) Extended Partnership and received funding from the European Union Next-Generation EU (PIANO NAZIONALE DI RIPRESA E RESILIENZA (PNRR) – MISSIONE 4 COMPONENTE 2, INVESTIMENTO 1.3 – D.D. 1551.11–10−2022, PE00000004). This manuscript reflects only the authors' views and opinions, neither the European Union nor the European Commission can be considered responsible for them.

Appendix A. Supporting information

Supplementary data associated with this article can be found in the online version at doi:10.1016/j.materresbull.2026.114305.

Data availability

Data will be made available on request.

References

[1] M.K. Ijaz, B. Zargar, K.E. Wright, J.R. Rubino, S.A. Sattar, Generic aspects of the airborne spread of human pathogens indoors and emerging air decontamination technologies, Am. J. Infect. Control. 44 (2016) S109–S120, https://doi.org/10.1016/j.ajic.2016.06.008.
[2] P. Azimi, B. Stephens, HVAC filtration for controlling infectious airborne disease transmission in indoor environments: Predicting risk reductions and operational costs, Build. Environ. 70 (2013) 150–160, https://doi.org/10.1016/j.buildenv.2013.08.025.
[3] M. Rezaei, R.R. Netz, Airborne virus transmission via respiratory droplets: effects of droplet evaporation and sedimentation, Curr. Opin. Colloid Interface Sci. 55 (2021) 101471, https://doi.org/10.1016/j.cocis.2021.101471.
[4] H. Li, X. Qian, Q. Wang, Heavy metals in atmospheric particulate matter: a comprehensive understanding is needed for monitoring and risk mitigation, Environ. Sci. Technol. 47 (2013) 13210–13211, https://doi.org/10.1021/es404751a.
[5] H. Myung, Y.S. Joung, Contribution of particulates to airborne disease transmission and severity: a review, Environ. Sci. Technol. 58 (2024) 6846–6867, https://doi.org/10.1021/acs.est.3c08835.
[6] X. Zhou, X. Zhou, C. Wang, H. Zhou, Environmental and human health impacts of volatile organic compounds: a perspective review, Chemosphere 313 (2023) 137489, https://doi.org/10.1016/j.chemosphere.2022.137489.
[7] T.Z. Maung, J.E. Bishop, E. Holt, A.M. Turner, C. Pfrang, Indoor air pollution and the health of vulnerable groups: a systematic review focused on particulate matter (PM), volatile organic compounds (VOCs) and their effects on children and people with pre-existing lung disease, Int. J. Environ. Res. Public. Health 19 (2022) 8752, https://doi.org/10.3390/ijerph19148752.
[8] S. Han, J. Kim, S.H. Ko, Advances in air filtration technologies: structure-based and interaction-based approaches, Mater. Today Adv. 9 (2021) 100134, https://doi.org/10.1016/j.mtadv.2021.100134.
[9] J.T. Walker, A. Jhutty, S. Parks, C. Willis, V. Copley, J.F. Turton, P.N. Hoffman, A. M. Bennett, Investigation of healthcare-acquired infections associated with Pseudomonas aeruginosa biofilms in taps in neonatal units in Northern Ireland, J. Hosp. Infect. 86 (2014) 16–23, https://doi.org/10.1016/j.jhin.2013.10.003.
[10] S. Mobasser, Y. Wager, T.M. Dittrich, Indoor air purification of volatile organic compounds (VOCs) using activated carbon, zeolite, and organosilica sorbents, Ind. Eng. Chem. Res. 61 (2022) 6791–6801, https://doi.org/10.1021/acs.iecr.1c04732.
[11] D. Kallo, Applications of natural zeolites in water and wastewater treatment, Rev. Mineral. Geochem. 45 (2001) 519–550, https://doi.org/10.2138/rmg.2001.45.15.

[12] N. Grifasi, B. Ziantoni, D. Fino, M. Piumetti, Fundamental properties and sustainable applications of the natural zeolite clinoptilolite, Environ. Sci. Pollut. Res. (2024), https://doi.org/10.1007/s11356-024-33656-5.

[13] L. Akhigbe, S. Ouki, D. Saroj, X.M. Lim, Silver-modified clinoptilolite for the removal of Escherichia coli and heavy metals from aqueous solutions, Environ. Sci. Pollut. Res. 21 (2014) 10940–10948, https://doi.org/10.1007/s11356-014-2888-6.

[14] F. Gattucci, M. Lallukka, N. Grifasi, M. Piumetti, M. Miola, Tannic acid-assisted green functionalization of Clinoptilolite: A step-by-step characterization of silver nanoparticles in situ reduction, S0272884225001622, Ceram. Int. (2025), https://doi.org/10.1016/j.ceramint.2025.01.151.

[15] A. Dziedzicka, B. Sulikowski, M. Ruggiero-Mikołajczyk, Catalytic and physicochemical properties of modified natural clinoptilolite, Catal. Today 259 (2016) 50–58, https://doi.org/10.1016/j.cattod.2015.04.039.

[16] P. Dutta, B. Wang, Zeolite-supported silver as antimicrobial agents, Coord. Chem. Rev. 383 (2019) 1–29, https://doi.org/10.1016/j.ccr.2018.12.014.

[17] N. Mintcheva, M. Panayotova, G. Gicheva, O. Gemishev, G. Tyuliev, Effect of exchangeable ions in natural and modified zeolites on Ag content, Ag nanoparticle formation and their antibacterial activity, Materials 14 (2021) 4153, https://doi.org/10.3390/ma14154153.

[18] Q.L. Feng, J. Wu, G.Q. Chen, F.Z. Cui, T.N. Kim, J.O. Kim, A mechanistic study of the antibacterial effect of silver ions onEscherichia coli andStaphylococcus aureus, J. Biomed. Mater. Res. 52 (2000) 662–668, https://doi.org/10.1002/1097-4636(20001215)52:4%253C662::AID-JBM10%253E3.0.CO;2-3.

[19] W.K. Jung, H.C. Koo, K.W. Kim, S. Shin, S.H. Kim, Y.H. Park, Antibacterial activity and mechanism of action of the silver ion in *Staphylococcus aureus* and *Escherichia coli*, Appl. Environ. Microbiol. 74 (2008) 2171–2178, https://doi.org/10.1128/AEM.02001-07.

[20] S. Tang, J. Zheng, Antibacterial activity of silver nanoparticles: structural effects, Adv. Healthc. Mater. 7 (2018) 1701503, https://doi.org/10.1002/adhm.201701503.

[21] A. Luceri, R. Francese, D. Lembo, M. Ferraris, C. Balagna, Silver nanoparticles: review of antiviral properties, mechanism of action and applications, Microorganisms 11 (2023) 629, https://doi.org/10.3390/microorganisms11030629.

[22] A. Top, S. Ülkü, Silver, zinc, and copper exchange in a Na-clinoptilolite and resulting effect on antibacterial activity, Appl. Clay Sci. 27 (2004) 13–19, https://doi.org/10.1016/j.clay.2003.12.002.

[23] B. Concepción-Rosabal, G. Rodríguez-Fuentes, N. Bogdanchikova, P. Bosch, M. Avalos, V.H. Lara, Comparative study of natural and synthetic clinoptilolites containing silver in different states, Microporous Mesoporous Mater. 86 (2005) 249–255, https://doi.org/10.1016/j.micromeso.2005.07.027.

[24] R.N.M. Missengue, N.M. Musyoka, G. Madzivire, O. Babajide, O.O. Fatoba, M. Tuffin, L.F. Petrik, Leaching and antimicrobial properties of silver nanoparticles loaded onto natural zeolite clinoptilolite by ion exchange and wet impregnation, J. Environ. Sci. Health Part. A 51 (2016) 97–104, https://doi.org/10.1080/10934529.2015.1087731.

[25] M.I. Panayotova, N.N. Mintcheva, O.T. Gemishev, G.T. Tyuliev, G.D. Gicheva, L.P. Djerahov, Preparation and antimicrobial properties of silver nanoparticles supported by natural zeolite clinoptilolite, (n.d.).

[26] A. Ruíz-Baltazar, R. Pérez, Kinetic adsorption study of silver nanoparticles on natural zeolite: experimental and theoretical models, Appl. Sci. 5 (2015) 1869–1881, https://doi.org/10.3390/app5041869.

[27] H. Irvani, M. Pour, A. Vahidi, S. Arezoomandan, H.-F. Abady, Removal of toluene vapors from the polluted air with modified natural zeolite and titanium dioxide nanoparticles, Med. Gas. Res. 8 (2018) 91, https://doi.org/10.4103/2045-9912.241074.

[28] T.L. Rakitskaya, T.A. Kiose, K.O. Golubchik, A.A. Ennan, V.Y. Volkova, Acid-modified clinoptilolite as a support for palladium–copper complexes catalyzing carbon monoxide oxidation with air oxygen, Chem. Cent. J. 11 (2017) 28, https://doi.org/10.1186/s13065-017-0256-6.

[29] D.A. Morgott, Anthropogenic and biogenic sources of Ethylene and the potential for human exposure: a literature review, Chem. Biol. Interact. 241 (2015) 10–22, https://doi.org/10.1016/j.cbi.2015.08.012.

[30] A. Vanker, P.M. Nduru, W. Barnett, F.S. Dube, P.D. Sly, R.P. Gie, M.P. Nicol, H. J. Zar, Indoor air pollution and tobacco smoke exposure: impact on nasopharyngeal bacterial carriage in mothers and infants in an African birth cohort study, ERJ Open. Res. 5 (2019) 00052–02018, https://doi.org/10.1183/23120541.00052-2018.

[31] G. Adamkiewicz, World Health Organization (Eds.), WHO guidelines for indoor air quality: selected pollutants, World Health Organization, Regional Office for Europe, Copenhagen, Denmark, 2010.

[32] N. Keller, M.-N. Ducamp, D. Robert, V. Keller, Ethylene removal and fresh product storage: a challenge at the frontiers of chemistry. toward an approach by photocatalytic oxidation, Chem. Rev. 113 (2013) 5029–5070, https://doi.org/10.1021/cr900398v.

[33] Y. Qi, C. Li, H. Li, H. Yang, J. Guan, Elimination or removal of ethylene for fruit and vegetable storage via low-temperature catalytic oxidation, J. Agric. Food Chem. 69 (2021) 10419–10439, https://doi.org/10.1021/acs.jafc.1c02868.

[34] E. Bozzola, R. Agostiniani, L. Pacifici Noja, J. Park, P. Lauriola, T. Nicoletti, D. Taruscio, G. Taruscio, A. Mantovani, The impact of indoor air pollution on children's health and well-being: the experts' consensus, Ital. J. Pediatr. 50 (2024) 69, https://doi.org/10.1186/s13052-024-01631-y.

[35] P.A. Bolla, S. Huggias, M.A. Serradell, J.F. Ruggera, M.L. Casella, Synthesis and catalytic application of silver nanoparticles supported on Lactobacillus kefiri S-Layer Proteins, Nanomaterials 10 (2020) 2322, https://doi.org/10.3390/nano10112322.

[36] T.T.T.L. Hoang, N. Insin, N. Sukpirom, Catalytic activity of silver nanoparticles anchored on layered double hydroxides and hydroxyapatite, Inorg. Chem. Commun. 121 (2020) 108199, https://doi.org/10.1016/j.inoche.2020.108199.

[37] C. Balagna, S. Perero, F. Bosco, C. Mollea, M. Irfan, M. Ferraris, Antipathogen nanostructured coating for air filters, Appl. Surf. Sci. 508 (2020) 145283, https://doi.org/10.1016/j.apsusc.2020.145283.

[38] N. Mansouri, N. Rikhtegar, H.A. Panahi, F. Atabi, B.K. Shahraki, Porosity, characteriza-tion and structural properties of natural zeolite – clinoptilolite – as a sorbent, Environ. Prot. Eng. 39 (2013), https://doi.org/10.37190/epe130111.

[39] M. Sprynskyy, R. Golembiewski, G. Trykowski, B. Buszewski, Heterogeneity and hierarchy of clinoptilolite porosity, J. Phys. Chem. Solids 71 (2010) 1269–1277, https://doi.org/10.1016/j.jpcs.2010.05.006.

[40] Petre Melikishvili Institute of Physical & Organic Chemistry TSU Georgia, V. G. Tsitsishvili, N.M. Dolaberidze, Petre Melikishvili Institute of Physical & Organic Chemistry TSU Georgia, M.O. Nijaradze, Petre Melikishvili Institute of Physical & Organic Chemistry TSU Georgia, N.A. Mirdzveli, Petre Melikishvili Institute of Physical & Organic Chemistry TSU Georgia, Z.S. Amiridze, Petre Melikishvili Institute of Physical & Organic Chemistry TSU Georgia, Bactericidal adsorbents obtained by ion exchange modification of natural phillipsite, Him. Fiz. Ta Tehnol. Poverhni 10 (2019) 327–339, https://doi.org/10.15407/hftp10.04.327.

[41] J. Liu, Scanning transmission electron microscopy and its application to the study of nanoparticles and nanoparticle systems, Microscopy 54 (2005) 251–278, https://doi.org/10.1093/jmicro/dfi034.

[42] M.A. Asoro, P.J. Ferreira, D. Kovar, situ transmission electron microscopy and scanning transmission electron microscopy studies of sintering of Ag and Pt nanoparticles, Acta Mater. 81 (2014) 173–183, https://doi.org/10.1016/j.actamat.2014.08.028.

[43] E.L. Pavlova, E.P. Nenova, L.D. Yocheva, I.A. Ivanova, P.A. Georgiev, Antimicrobial and oxidative activities of different levels of silver-exchanged zeolites X and ZSM-5 and Their Ecotoxicity, Pharmaceuticals 17 (2024) 1586, https://doi.org/10.3390/ph17121586.

[44] P. Sen, J. Ghosh, A. Abdullah, P. Kumar, Vandana, Preparation of Cu, Ag, Fe and Al nanoparticles by the exploding wire technique, J. Chem. Sci. 115 (2003) 499–508, https://doi.org/10.1007/BF02708241.

[45] M.A.A. Hamid, H.A. Aziz, M.S. Yusoff, S.A. Rezan, Optimization and analysis of zeolite augmented electrocoagulation process in the reduction of high-strength ammonia in saline landfill leachate, Water 12 (2020) 247, https://doi.org/10.3390/w12010247.

[46] M. Thommes, K. Kaneko, A.V. Neimark, J.P. Olivier, F. Rodriguez-Reinoso, J. Rouquerol, K.S.W. Sing, Physisorption of gases, with special reference to the evaluation of surface area and pore size distribution (IUPAC Technical Report), Pure Appl. Chem. 87 (2015) 1051–1069, https://doi.org/10.1515/pac-2014-1117.

[47] E. Davarpanah, M. Armandi, S. Hernández, D. Fino, R. Arletti, S. Bensaid, M. Piumetti, CO_2 capture on natural zeolite clinoptilolite: effect of temperature and role of the adsorption sites, J. Environ. Manag. 275 (2020) 111229, https://doi.org/10.1016/j.jenvman.2020.111229.

[48] E.P. Favvas, C.G. Tsanaktsidis, A.A. Sapalidis, G.T. Tzilantonis, S.K. Papageorgiou, A.Ch Mitropoulos, Clinoptilolite, a natural zeolite material: Structural characterization and performance evaluation on its dehydration properties of hydrocarbon-based fuels, Microporous Mesoporous Mater. 225 (2016) 385–391, https://doi.org/10.1016/j.micromeso.2016.01.021.

[49] V.J. Inglezakis, M. Stylianou, M. Loizidou, Ion exchange and adsorption equilibrium studies on clinoptilolite, bentonite and vermiculite, J. Phys. Chem. Solids 71 (2010) 279–284, https://doi.org/10.1016/j.jpcs.2009.12.077.

[50] K.-J. Hwang, W.-S. Choi, S.-H. Jung, Y.-J. Kwon, S. Hong, C. Choi, J.-W. Lee, W.-G. Shim, Synthesis of zeolitic material from basalt rock and its adsorption properties for carbon dioxide, RSC Adv. 8 (2018) 9524–9529, https://doi.org/10.1039/C8RA00788H.

[51] O. Tammaro, G. Barrera, P. Allia, P. Tiberto, A. Marocco, M. Manzoli, B. Bonelli, G. Confalonieri, R. Arletti, M. Pansini, S. Esposito, Unravelling the role of the exchanged Ni amount in zeolites A and X for their thermal transformation into magnetic metal-ceramic nanocomposites, Ceram. Int. 49 (2023) 30536–30546, https://doi.org/10.1016/j.ceramint.2023.07.003.

[52] A. Gil, P. Grange, Application of the Dubinin-Radushkevich and Dubinin-Astakhov equations in the characterization of microporous solids, Colloids Surf. Physicochem. Eng. Asp. 113 (1996) 39–50, https://doi.org/10.1016/0927-7757(96)81455-5.

[53] Y. Wu, M. Song, Z. Chai, J. Huang, X. Wang, Integrating an Ag^0 –Ag^+ mediated $Ag_2Ta_4O_{11}$ /$Ag_8(Nb_{0.5}Ta_{0.5})_{26}O_{69}$ heterojunction to quickly decontaminate indoor gaseous formaldehyde under indoor temperature, humidity and sunlight irradiation conditions, Environ. Sci. Nano 7 (2020) 1831–1840, https://doi.org/10.1039/D0EN00202J.

[54] C. He, J. Cheng, X. Zhang, M. Douthwaite, S. Pattisson, Z. Hao, Recent advances in the catalytic oxidation of volatile organic compounds: a review based on pollutant sorts and sources, Chem. Rev. 119 (2019) 4471–4568, https://doi.org/10.1021/acs.chemrev.8b00408.

[55] N. Mintcheva, M. Panayotova, G. Gicheva, O. Gemishev, G. Tyuliev, Effect of exchangeable ions in natural and modified zeolites on Ag content, Ag nanoparticle formation and their antibacterial activity, Materials 14 (2021) 4153, https://doi.org/10.3390/ma14154153.

[56] R. Mohammad Al Soubaihi, K. Mohammad Saoud, J. Dutta, Low-temperature CO oxidation by silver nanoparticles in silica aerogel mesoreactors, Chem. Eng. J. 455 (2023) 140576, https://doi.org/10.1016/j.cej.2022.140576.

[57] C.W. Lopes, J. Martinez-Ortigosa, K. Góra-Marek, K. Tarach, J.A. Vidal-Moya, A. E. Palomares, G. Agostini, T. Blasco, F. Rey, Zeolite-driven Ag species during redox treatments and catalytic implications for SCO of NH_3, J. Mater. Chem. A 9 (2021) 27448–27458, https://doi.org/10.1039/D1TA09625G.
[58] G. Bagnasco, P. Ciambelli, E. Czaran, J. Papp, G. Russo, Oxidation of ethylene on silver-loaded natural zeolites. Stud. Surf. Sci. Catal, Elsevier, 1982, pp. 275–282, https://doi.org/10.1016/S0167-2991(09)61017-X.
[59] I. López-Hernández, C. García, V. Truttmann, S. Pollitt, N. Barrabés, G. Rupprechter, F. Rey, A.E. Palomares, Evaluation of the silver species nature in Ag-ITQ2 zeolites by the CO oxidation reaction, Catal. Today 345 (2020) 22–26, https://doi.org/10.1016/j.cattod.2019.12.001.
[60] P. Poldorn, Y. Wongnongwa, S. Namuangruk, N. Kungwan, V.B. Golovko, B. Inceesungvorn, S. Jungsuttiwong, Theoretical mechanistic study of CO catalytic oxidation by O2 on an ultra-small 13-atom bimetallic Ag7Au6 cluster, Appl. Catal. Gen. 595 (2020) 117505, https://doi.org/10.1016/j.apcata.2020.117505.
[61] M. Lamoth, M. Plodinec, L. Scharfenberg, S. Wrabetz, F. Girgsdies, T. Jones, F. Rosowski, R. Horn, R. Schlögl, E. Frei, Supported Ag Nanoparticles and Clusters for CO Oxidation: Size Effects and Influence of the Silver–Oxygen Interactions, ACS Appl. Nano Mater. 2 (2019) 2909–2920, https://doi.org/10.1021/acsanm.9b00344.
[62] D. Tang, Z. Chen, J. Hu, G. Sun, S. Lu, C. Hu, CO oxidation catalyzed by silver nanoclusters: mechanism and effects of charge, Phys. Chem. Chem. Phys. 14 (2012) 12829, https://doi.org/10.1039/c2cp41845b.
[63] L. Kvitek, A. Panacek, R. Prucek, J. Soukupova, M. Vanickova, M. Kolar, R. Zboril, Antibacterial activity and toxicity of silver – nanosilver versus ionic silver, J. Phys. Conf. Ser. 304 (2011) 012029, https://doi.org/10.1088/1742-6596/304/1/012029.
[64] T.C. Dakal, A. Kumar, R.S. Majumdar, V. Yadav, Mechanistic basis of antimicrobial actions of silver nanoparticles, Front. Microbiol. 7 (2016), https://doi.org/10.3389/fmicb.2016.01831.
[65] Z.-J. Jiang, C.-Y. Liu, L.-W. Sun, Catalytic properties of silver nanoparticles supported on silica spheres, J. Phys. Chem. B 109 (2005) 1730–1735, https://doi.org/10.1021/jp046032g.